Electronic Supplementary Material (ESI) for Journal of Materials Chemistry A.

Supporting Information

Indole-based Conjugated Microporous Polymer: A New and Stable Lithium Storage Anode with High-Capacity and Long-life Induced by Cation-π Interaction and N-rich Aromatic Structure

Wenxuan Wei,†[a] Guanjun Chang,†*[ab] Yewei Xu[a] and Li Yang*[ab]

[a] State Key Laboratory of Environment-friendly Energy Materials & School of Material Science and Engineering, Engineering, National Engineering Technology Center for Insulation Materials, Southwest University of Science and Technology, Mianyang, 621010, P. R. China

[b] Department of Chemical and Biomolecular Engineering, University of Pennsylvania, Philadelphia, Pennsylvania, 19104, United States.

*To whom correspondence should be addressed: Guanjun Chang, Email: gjchang@mail.ustc.edu.cn; Li Yang, Email: yanglichem628@126.com.

Table of contents

1 Main materials and measurements

1.1 Materials

Indole, 3-indoleacetamide and potassium tert-butoxide were purchased from Aladdin® and used without further purification. Oxalyl chloride and sodium methylate were purchased from Macklin® and used without further purification. The rest materials and reagents were obtained from different commercial sources and used without further purification.

1.2 Characterization Techniques

The thermal properties of the polymer were evaluated using thermogravimetric analysis on a simultaneous thermal analysis instrument (SDT Q600) over the temperature ranging from 20 to 800 ^{o}C under a nitrogen atmosphere with a heating rate of 10 °C min^{-1}. Elemental analysis was carried out on Vario EL CUBE Elemental Analyzer. FT-IR spectra were collected in transmission on a 380FT-IR spectrometer (Thermo Electron, US) using KBr disks. The solid state ^{13}C CP/MAS NMR measurement was carried out on a Bruker Avance 600. The microscopic features of the sample were carried out on a field-emission scanning electron microscopy (FESEM) (Ultra 55). PXRD measurement was carried out on X-ray diffractometer (X'Pert PRO). Surface areas and pore size distributions were measured by nitrogen adsorption and desorption at 77.3 K using a Quantachrome automated adsorption analyzer. Pore size distributions and pore volumes were derived from the adsorption branches of the isotherms using NL-DFT. Samples were degassed at 180°C for 12 h under vacuum (10-5 bar) before analysis.

1.3 Simulation Method

MD simulation was performed using the amorphous cell module of Materials Studio (Accelrys Software Inc.) with a dreiding force field whose intermolecular parameters were optimized using quantum mechanics. The free energy of the reactants and products are calculated based on DFT calculation with B3LYP methods, using the

Gaussian-09 package.

1.4 Batteries Fabrication and Electrochemical Measurements

The CR2016 coin-type cells were assembled in an argon-filled glovebox, where both moisture and oxygen levels were less than 1 ppm. The electrodes were fabricated by mixing of 50 wt% active material PBIM with acetylene black (40 wt%) and polyvinylidene fluoride (PVDF, 10 wt%) in n-methyl-2-pyrrolidone (NMP) solvent, and then pasted onto the copper foils. The electrodes were cut into disks with a diameter of 14 mm and the mass loading of 0.6 mg cm^{-2} for the active material. Lithium foils were used as counter electrodes and macroporous polypropylene film (Celgard 2400) as the separator. The electrolyte solution was made of 1 M $LiPF_6$ in ethylene carbonate (EC)/diethyl carbonate (DEC) (1/1, w/w). The galvanostatic charge and discharge measurements were carried out by the NEWARE-BTS-5 V/5 mA testing instrument (Neware Co., Ltd., Shenzhen, China) in a voltage ranging from 0 to 3.0 V with the current rates of 0.05, 0.1, 0.3, 0.5, 1, 2, and 2.5 C mA g^{-1} at room temperature. CV measurements were carried out on a CHI660E electrochemical workstation (Chenhua Co., Ltd., Shanghai, China) at scan rates of 0.1 mV s^{-1} at room temperature.

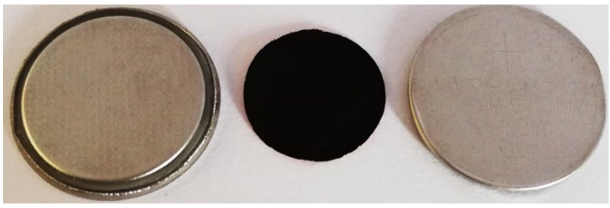

Figure S1 Photograph of the assembled CR2016 coin-type cells

2 Synthesis of monomer and polymer.

2.1 Synthesis and characterizations of 3,4-bisindolylmaleimide.[S1]

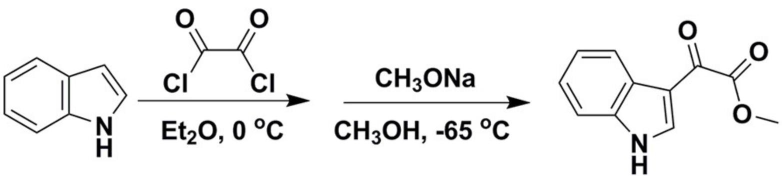

Scheme S1 Synthetic route of methyl-3-indoleglyoxylate.

A three-necked flask equipped with a magnetic stirrer and two addition funnels was charged with indole (10mmol) and 15 mL of diethyl ether. Oxalyl chloride (10mmol) was added dropwise to the solution at 0 °C under nitrogen in 0.5 h. Yellow precipitate were formed and the reaction mixture was stirred for another 0.5 h. The reaction mixture was cooled to -20 °C, then sodium methylate (25% solution in methanol, 1,08 g) was added dropwise to the reaction mixture in 1 h. After that the reaction mixture was warmed to 0 °C and 50 mL of water was added. The precipitate were filtered, washed with water several times, and then dried at 60 °C under vacuum. Yield: 90%.

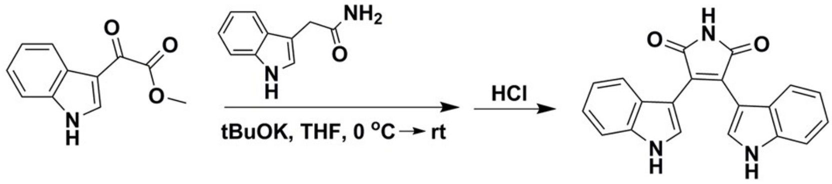

Scheme S2 Synthetic route of 3,4-bisindolylmaleimide.

A three-necked flask equipped with a magnetic stirrer and an addition funnel was charged with 3-indoleacetamide (10 mmol), methyl indolyl-3-glyoxylate (10 mmol) and 80 mL of tetrahydrofuran. A solution of potassium tert-butoxide (30 mmol) in 30 mL of tetrahydrofuran was added dropwise to the reaction mixture at 0 °C under nitrogen in 1.5 h. Then the reaction mixture was warmed to room temperature and stirred for 3 h. A solution of Hydrochloric acid (35% in water, 15 mL) was 1 h. Then 200 mL of ethyl acetate and 100 mL of water were added and stirred for dissolving. The organic phase was separated, washed with water several times until neutral, and then washed with brine once, dried over anhydrous sodium sulfate. The sodium sulfate was filtered and the solution was concentrated. The product was purified by flash chromatography (ethyl acetate/Petroleum ether= 1:3). The pure product of 3,4-bisindolylmaleimide was obtained as a red crystal.Yield: 68%; M.p. 204 °C; ^{1}H-NMR (400 MHz, $(CD_3)_2S=O$): δ = 6.63 (m, 2H, ArH), 6.80 (d, 2H, *J* = 8.5 Hz, ArH), 6.97 (m, 2H, ArH), 7.36 (d, 2H, *J* = 8 Hz, ArH), 7.74 (d, 2H, ArH), 10.93 (s, 1H, maleimide NH), 11.67 (s, 2H, indole NH) ppm. ^{13}C NMR(100 MHz, $(CD_3)_2S=O$): δ = 173.10, 136.35, 129.49, 128.08, 125.63, 122.19, 121.17, 119.36, 112.08, 105.89 ppm.

FT-IR spectrum(KBr pellet, cm^{-1}): 3417, 3323, 1698, 1422, 1339. Anal. Calcd. For $C_{20}H_{13}O_2N_3$: C, 73.38; H, 4.00; N, 12.84; O, 9,78. Found: C, 72.58; H, 4.11; N, 12.46; O, 9,79.

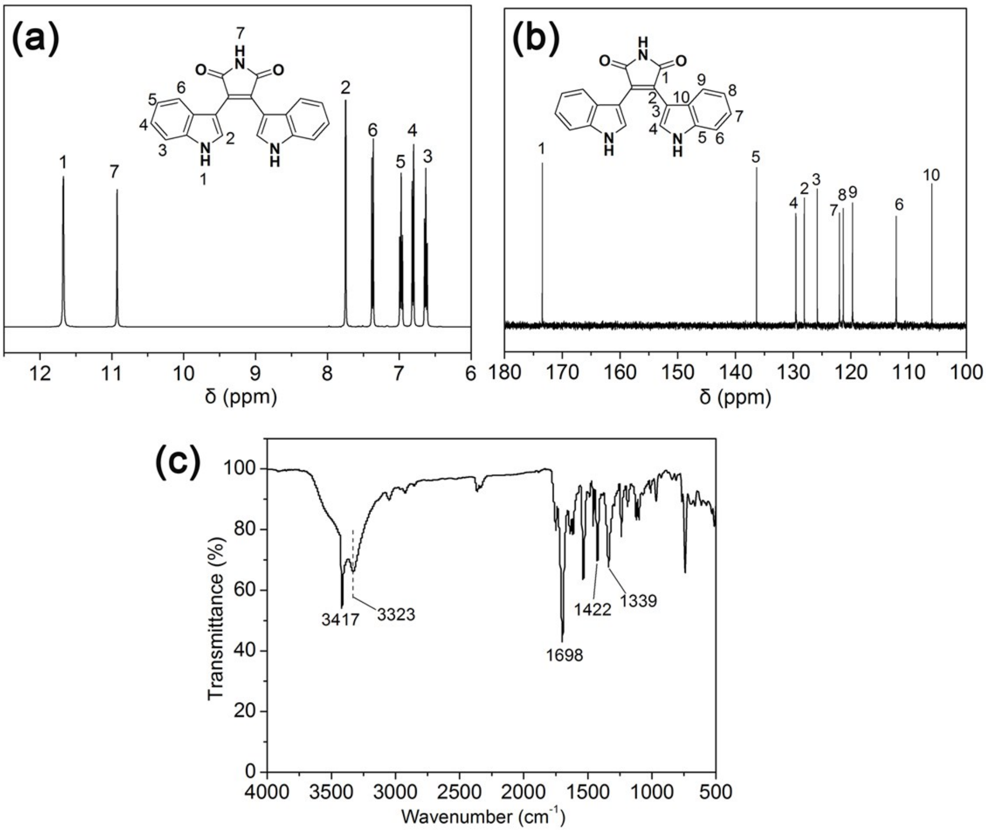

Figure S2 Characterizations of compound bisindolylmaleimide (BIM). (A) ^{1}H NMR, (B) ^{13}C NMR, (C) FTIR.

2.2 Synthesis of polymer

The monomer 3,4-bisindolylmaleimide (1 mmol, 1 equiv.) was dissolved in 60 mL of chloroform, while an oxidant anhydrous $FeCl_3$ (6 mmol, 6 equiv.) was dissolved in 15 mL of nitromethane (CH_3NO_2). The mixture was stirred at room temperature for 24 h, and then 100 mL of methanol was added. The resulting precipitate was collected by filtration and washed with methanol three times and 2 M HCl solution. After extracted in a Soxhlet extractor with methanol and THF for 24 hours at reflux, respectively, the product was collected and dried in vacuum oven at 80 ^{o}C for 24 hours (yield, 83%).

3 Powder X-ray diffraction of PBIM

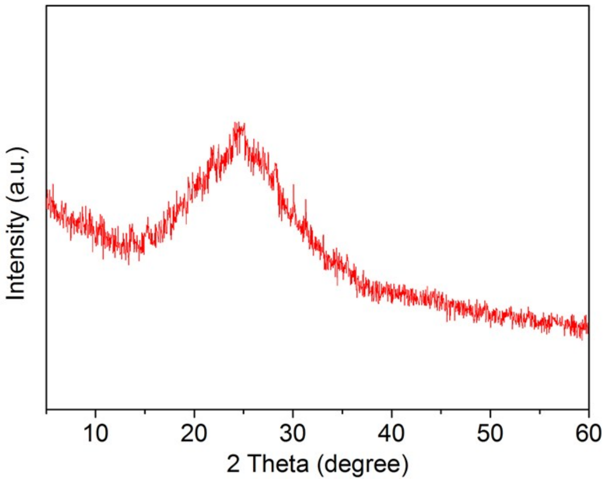

Figure S3 X-Ray diffraction patterns of PBIM.

4 Thermal behaviors of the PBIM

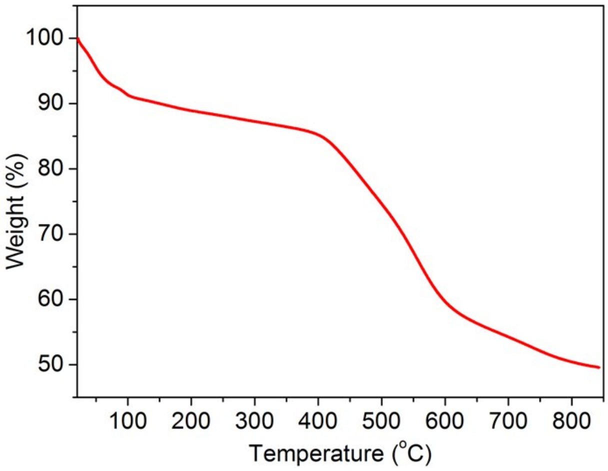

Figure S4 TGA curves of PBIM in nitrogen atmosphere.

5 Reversible Li-ion insertion/extraction mechanism

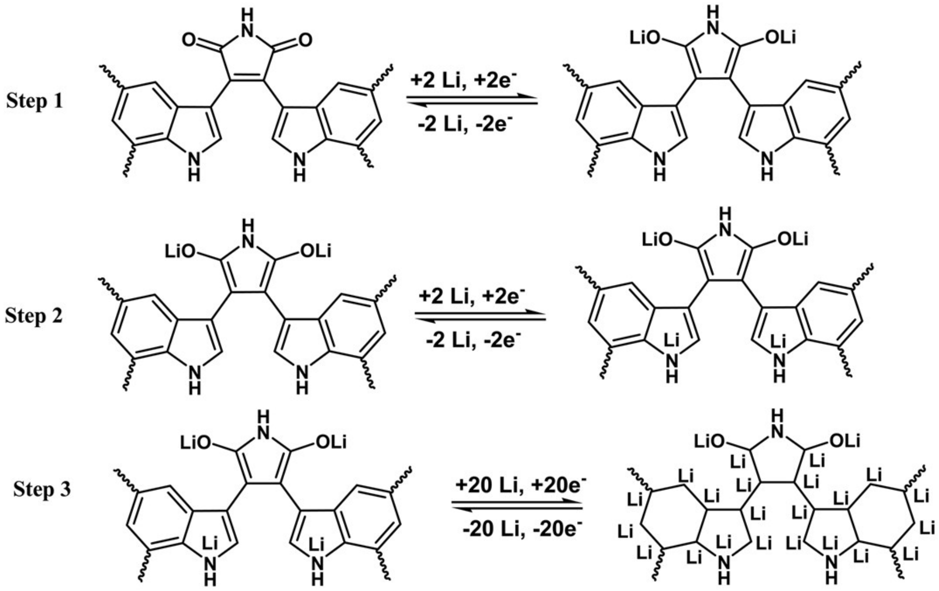

Scheme S3 Reversible Li-ion insertion/extraction mechanism of PBIM.

In the Li-ion insertion/extraction process, carbonyl oxygen of maleimide segments and indole rings both have contribution to capacity. Besides possible electrochemical lithiation at two carbonyl oxygen and aromatic nitrogen of PBIM (step 1 and 2), we believe that a maximum of twenty Li ions may be added on the unsaturated carbons by forming a PBIM-Li complex (step 3), which has also been shown for some multiring aromatic compounds. As a result, a total of 24 lithium ions can be stored in one BIM active unit. Therefore, the theoretical capacity of PBIM was calculated to be 1967 mAh g^{-1}.

6 Theoretical calculations

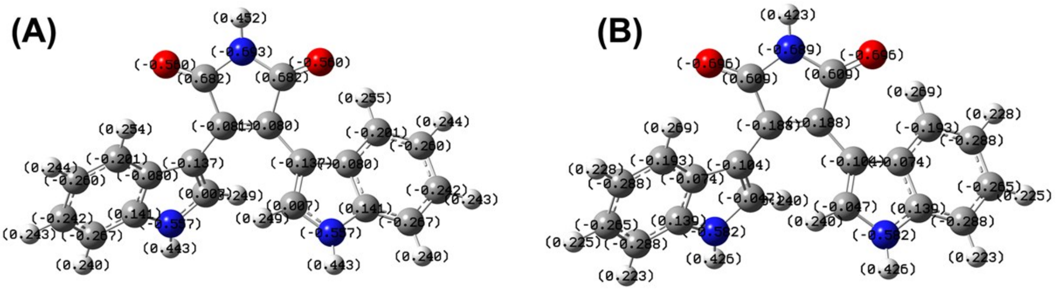

Figure S5 The natural bond orbital (NBO) charge distributions of (A) the neutral state and (B) monoanion state

To further understand our results, additional theoretical calculations were performed with the Gaussian 09 program. As shown in Figure S5, The natural bond orbital (NBO) charge analysis was performed to investigate the redox reaction . When the neutral PBIM was reduced to monoanion state, the electron densities of oxygen atoms drastically increased (for O from -0.560 to -0.696). The increased electron densities in carbonyl oxygen will be favorably to bind with the electron-deficient Li cation. Additionally, the electron densities of the nitrogen atoms of indole ring also increased (for N atoms in indole ring from -0.557 to -0.582). Therefore, the N atoms in indole ring are also the binding sites for Li^+. There is almost no change in the electron density of N atom of amide group, which indicated the N13 atom of amide group does not participate in the redox reaction.

7 The first charge/discharge profile of PBIM-based LIBs

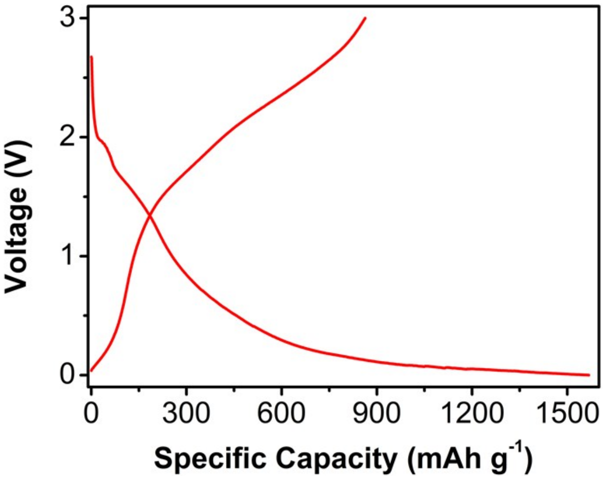

Figure S6 The first charge/discharge profile of PBIM-based LIBs under 50 mA g^{-1}.

8 Performance comparison

Table S1. A comparison of cyclic stability of our conjugated microporous polymer PBIM anodes to some of other organic microporous anode materials.

Anode materials	Performance	Potential window	Reference
Poly(bisindolylmaleimide) (PBIM)	510 mAh g^{-1} after 1000 cycles at 1000 mA g^{-1}	0.0-3.0 V	This study
Bipolar porous polymeric frameworks (BPPF)	25 mAh g^{-1} after 1000 cycles at 1000 mA g^{-1}	0.0-3.5 V	[S2]
Conjugated microporous Polytetra(2-Thienyl)ethylene (PTTE)	585 mA h g^{-1} after 100 cycles at 500 mA g^{-1}	0.0-3.0 V	[S3]
Bicarbozole-based redox-active COF (Cz-COF1)	236 mAh g^{-1} after 400 cycles at 200 mA g^{-1}	0.005-3.0 V	[S4]

Three-Dimensional Arylene Diimide Frameworks (PDI-Tc)	45 mAh g^{-1} after 500 cycles at 2C (192.8 mA g^{-1})	1.7-3.3 V	[S5]
Porous polyimides (PI-3)	1.5－4.2 V	57.9 mA h g^{-1} after 500 cycles at 25 mA g^{-1}	[S6]
N-doped porous carbon materials (NPC-2)	0.005-3.0 V	488 mA h g^{-1} after 100 cycles at 100 mA g^{-1}	[S7]
Conjugated covalent organic frameworks (N2-COF)	593 mA h g^{-1} after 500 cycles at 1C (1000 mA g^{-1})	0.05-3.0 V	[S8]
Nitrogen/sulfur co-doped carbon （NS$_{1/3}$）	864 mA h g^{-1} after 50 cycles at 100 mA g^{-1}	0.01-3.0 V	[S9]

Supporting References

[S1] Q. Zhang, G. Chang and L. Zhang. Synthesis and properties of novel heat-resistant fluorescent conjugated polymers with bisindolylmaleimide. Chinese Chem. Lett., 2018, 29, 513-516.

[S2] K. Sakaushi, E. Hosono , G. Nickerl, H. Zhou, S. Kaskel and J. Eckert. Bipolar porous polymeric frameworks for low-cost, high-power, long-life all-organic energy storage devices. J. Power Sources, 2014, 245, 553-556.

[S3] X. Wang, C. Zhang, Y. Xu, Q. He, P. Mu, Y. Chen, J. Zeng, F. Wang and J.-X. Jiang. Conjugated Microporous Polytetra(2-Thienyl)ethylene as High Performance Anode Material for Lithiumand Sodium-Ion Batteries. Macromol. Chem. Phys., 2018, 219, 1700524.

[S4] S. Feng, H. Xu, C. Zhang, Y. Chen, J. Zeng, D. Jiang and J.-X. Jiang. Bicarbozole-based redox-active covalent organic frameworks for ultrahigh-performance energy storage. Chem. Commun., 2017,53, 11334-11337.

[S5] T. B. Schon, A. J. Tilley, E. L. K. and D. S. Seferos. Three-Dimensional Arylene Diimide Frameworks for Highly Stable Lithium Ion Batteries. ACS Appl. Mater. Interfaces, 2017, 9, 15631-15637.

[S6] D. Tian, H.-Z. Zhang, Da-Shuai Zhang, Z. Chang, J. Han, X.-P. Gao and X.-H. Bu. Li-ion storage and gas adsorption properties of porous polyimides (PIs). RSC Adv., 2014, 4, 7506-7510.

[S7] X. Zhang, G. Zhu, M. Wang, J. Li, T. Lu, and L. Pan. Covalent-organic-frameworks derived N-doped porous carbon materials as anode for superior long-life cycling lithium and sodium ion batteries. Carbon, 2017,116, 686-694.

[S8] L. Bai, Q. Gao and Y. Zhao. Two fully conjugated covalent organic frameworks as anode materials for lithium ion batteries. J. Mater. Chem. A, 2016, 4, 14106-14110.

[S9] Z. Qiu, Y. Lin, H. Xin, P. Han, D. Li, B. Yang, P. Li , S. Ullah, H. Fan, C. Zhu, J. Xu. Ultrahigh level nitrogen/sulfur co-doped carbon as high performance anode materials for lithium-ion batteries. Carbon, 2018, 126, 85-92.